Method of carrier-free delivery of therapeutic RNA importable into human mitochondria: Lipophilic conjugates with cleavable bonds

Ilya Dovydenko, Ivan Tarassov, Alya Venyaminova, Nina Entelis

Method of carrier-free delivery of therapeutic RNA importable into human mitochondria: lipophilic conjugates with cleavable bonds.

Ilya Dovydenko[1,2], Ivan Tarassov [1], Alya Venyaminova[2], Nina Entelis [1]*

[1] Department of Molecular and Cellular Genetics, UMR Génétique Moléculaire, Génomique, Microbiologie (GMGM), Strasbourg University - CNRS , Strasbourg 67084 France;
[2] Laboratory of RNA Chemistry, Institute of Chemical Biology and Fundamental Medicine, Siberian Branch of Russian Acadadmy of Sciences, Novosibirsk Russia

*Corresponding author, UMR 7156, 4, Allée Konrad Roentgen 67081 STRASBOURG Cedex , France; n.entelis@unistra.fr

ABSTRACT

Defects in mitochondrial DNA often cause neuromuscular pathologies, for which no efficient therapy has yet been developed. MtDNA targeting nucleic acids might therefore be promising therapeutic candidates. Nevertheless, mitochondrial gene therapy has never been achieved because DNA molecules can not penetrate inside mitochondria *in vivo*. In contrast, some small non-coding RNAs are imported into mitochondrial matrix, and we recently designed mitochondrial RNA vectors that can be used to address therapeutic oligoribonucleotides into human mitochondria. Here we describe an approach of carrier-free targeting of the mitochondrially importable RNA into living human cells. For this purpose, we developed the protocol of chemical synthesis of oligoribonucleotides conjugated with cholesterol residue through cleavable covalent bonds. Conjugates containing pH-triggered hydrazone bond were stable during the cell transfection procedure and rapidly cleaved in acidic endosomal cellular compartments. RNAs conjugated to cholesterol through a hydrazone bond were characterized by efficient carrier-free cellular uptake and partial co-localisation with mitochondrial network. Moreover, the imported oligoribonucleotide designed to target a pathogenic point mutation in mitochondrial DNA was able to induce a decrease in the proportion of mutant mitochondrial genomes. This newly developed approach can be useful for a carrier-free delivery of therapeutic RNA into mitochondria of living human cells.

Keywords: cell delivery; RNA therapeutics; RNA conjugates; mitochondrial drug delivery; mitochondrial diseases; antireplicative RNA.

Introduction

Small RNA molecules are increasingly used in clinical applications. RNA-based therapeutics include inhibitors of mRNA translation, agents of RNA interference, ribozymes and aptamers binding various molecular targets [1, 2]. Recently, we developed mitochondrial RNA vectors that can be used to address therapeutic oligoribonucleotides into human mitochondria [3, 4]. To date, >250 human diseases, mostly neuromuscular and neurodegenerative, were shown to be caused by defects in mitochondrial DNA (mtDNA) [5]. The majority of these mutations are heteroplasmic, meaning that mtDNA coexists in two forms, wild type and mutated, in the same cell. The occurrence and severity of pathologic effects depend on the heteroplasmy

level, therefore, the shift in proportion between two types of mitochondrial genome could restore mitochondrial functions [6, 7]. Anti-replicative strategy aims to decrease the heteroplasmy level by targeting into mitochondria the RNA molecules able to affect the replication of mutant mtDNA. Recently, we demonstrated that small RNAs containing structural determinants for mitochondrial import (hairpin domains responsible for RNA mitochondrial targeting) and 20-nucleotide sequence corresponding to the mutated region of mtDNA, are able to anneal selectively to the mutated mitochondrial genomes. Capable to penetrate into mitochondria of cultured human cells, these RNAs induced a decrease of the proportion of mtDNA bearing pathogenic mutations [4, 8].

A factor that significantly limits biomedical application of RNAs is their inefficient delivery to target cells and tissues [9, 10]. Delivery of therapeutic RNAs in the complexes with cationic lipids has been characterized by high toxicity and inefficiency *in vivo* [10]. The conjugation of RNA with the ligands which can be internalized by natural transport mechanisms is a promising approach to overcome this problem [11].

To decrease the toxicity of cell transfection procedure and create an approach of targeting various anti-replicative RNAs into living human cells, we designed conjugates containing a cholesterol residue. Cholesterol is a natural lipid and an essential structural component of animal cell membranes, its efficiency as a transporter molecule and low toxicity were demonstrated by several research groups [12-14]. Nevertheless, cholesterol could stall the mitochondrial import of therapeutic anti-replicative RNA due to attachment to the mitochondrial membranes. To address this problem, we synthesized RNA molecules conjugated with cholesterol through cleavable covalent bonds. These linkages have been previously used to release drugs under specific conditions: cleavage of disulfide bonds is triggered by a mildly reducing intracellular environment; hydrazone bonds are pH - triggered linkers releasing the drug in acidic conditions of endosomes [15]. Here we describe the synthesis of oligoribonucleotides conjugated with cholesterol through cleavable covalent bonds and show that this approach can be used for a carrier-free transfection of human cells with anti-replicative RNA molecules addressing mtDNA mutations.

Materials and Methods

Chemical compounds

Thiol-Modifier C6 S-S, 5'-Aldehyde-Modifier C2, RNA phosphoramidites and solid supports for oligoribonucleotide synthesis were obtained from Glen Research; cholesteryl chloroformate, 6-aminohexanoic acid, cysteamine, chloroquine diphisphate salt and FITC

isomer I were purchased from Sigma-Aldrich; hydrazine hydrate - from Fluka; ATTO 565 N-succinimidyl ester from ATTO-TEC. Other chemicals were supplied by Merck, Acros and TCI. Solvents were supplied from Panreac.

Synthesis of chemical compounds

*6-(Cholesteryloxycarbonylamino)-hexanoic acid **(1)***

Compound **(1) (Fig. 1A, step i)** was synthesized as described in [16] with modifications. 6-Aminohexanoic acid (0.9 g, 6.6 mmol) was suspended in dry pyridine (15 ml), then chlorotrimethylsilane (3.3 ml, 26.4 mmol) was added dropwise at 0°C. The mixture was stirred until the solution became clear, then cholesteryl chloroformate (1 g, 2.2 mmol) was added and the reaction mixture was stirred for 3 h at room temperature. Pyridine was evaporated under reduced pressure, the residue was dissolved in dichloromethane (100 ml), washed with 0.7 M hydrochloric acid (50 ml) and saturated aqueous NaCl (50 ml). The organic phase was dried under anhydrous Na_2SO_4 and evaporated under reduced pressure. The residue was purified by Silicagel 60 Å 230–400 mesh (Sigma) column chromatography (CH_2Cl_2/EtOH, 0-30%) to obtain **(1)** with a yield 0.95 g (80%). ^{1}H NMR spectra were recorded on a Bruker AV-400 spectrometer with tetramethylsilane as an internal standard. H^1-NMR (400 MHz, $CDCl_3$, δ, ppm): 0.69 (s, 3H, H-18/19 cholesterol); 0.87 (d, 3H, H-26/27 cholesterol); 0.89 (d, 3H, H-26/27 cholesterol); 0.93 (d, 3H, H-21) cholesterol; 1.025 (s, 3H, H-18/19 cholesterol); 2.33 (t, 2H, -C<u>H</u>$_2$-COOH); 3.35 (dd, 2H, -C<u>H</u>$_2$-NH-,); 4.51 (m, 1H, H-3 cholesterol); 4.88 (t, 1H, -NH-,); 5.4 (d, 1H, H-6 cholesterol).

*Methyl 6-(cholesteryloxycarbonylamino)hexanoate **(2)***

Compound (**1**) (0.2 g, 0.37 mmol) was dissolved in dry dichloromethane (5 ml), phosphorus trichloride (13 µl, 0.149 mmol) was added (**Fig. 1A step ii**), the reaction mixture was stirred for 3h under argon at 50°C, then absolute methanol (1 ml) was added. The mixture was diluted by dichloromethane (45 ml) and washed with saturated aqueous $NaHCO_3$ (50 ml) and twice by water (50 ml). The organic phase was dried under anhydrous Na_2SO_4 and evaporated to oily residue. The product (**2**) was purified by Silica-gel column chromatography (CH_2Cl_2/EtOH, 0-2.5%) (yield 0.165 g, 80%).

H^1-NMR (400 MHz, $CDCl_3$, δ, ppm): 0.69 (s, 3H, H-18/19 cholesterol); 0.87 (d, 3H, H-26/27 cholesterol); 0.89 (d, 3H, H-26/27 cholesterol); 0.93 (d, 3H, H-21 cholesterol); 1.025 (s, 3H, H-18/19 cholesterol); 2.29 (t, 2H, -C<u>H</u>$_2$-C(O)OCH$_3$,); 3.35 (dd, 2H, -C<u>H</u>$_2$-NH-,); 3.65 (s, 3H, -CH$_2$-C(O)OC<u>H</u>$_3$,): 4.51 (m, 1H, H-3 cholesterol); 4.88 (t, 1H, -NH-,); 5.4 (d, 1H, H-6 cholesterol).

*Hydrazine 6-(cholesteryloxycarbonylamino)hexanoate (**3**)*

Hydrazine derivative **(3)** was synthesized by analogy with [17]. Compound **(2)** (0.1 g, 0.18 mmol) was dissolved in methanol (5 ml). Hydrazine monohydrate (1.25 mL, 49 mmol) was added dropwise (**Fig. 1A step iii)**, and the reaction mixture was left for 8 h at room temperature. Compound **(3)** was precipitated in cold water (100 ml), the precipitate was filtered off, washed with water and dried (yield, 0.089 g, 89%). H^1-NMR (400 MHz, $CDCl_3$, δ, ppm): 0.69 (s, 3H, H-18/19 cholesterol); 0.87 (d, 3H, H-26/27 cholesterol); 0.89 (d, 3H, H-26/27 cholesterol); 0.93 (d, 3H, H-21 cholesterol); 1.025 (s, 3H, H-18/19 cholesterol); 2.13 (t, 2H, -C$\underline{H}_2$-C(O)NH-NH_2,); 3.35 (dd, 2H, -C$\underline{H}_2$-NH-,); 3.85 (s, 2H, -CH_2-C(O)NH-N$\underline{H}_2$,): 4.51 (m, 1H, H-3 cholesterol); 4.88 (t, 1H, -NH-,); 5.4 (d, 1H, H-6 cholesterol); 6.75 (s, H, -CH_2-C(O)N$\underline{H}$-NH_2).

*2-(Pyridyldithio)-ethylamine **(4)***

Compound **(4)** (**Fig. 1B step i**) was synthesized as described in [18] with some modifications. The reaction was kept under argon atmosphere. Cysteamine (0.23g, 2 mmol) was dissolved in methanol (5 ml) and added dropwise to a stirred solution of 2,2'-dipyridyl disulfide (0.88g, 4 mmol) in methanol/acetic acid (1:25; 4 ml). The mixture was stirred at room temperature for 48 h and then evaporated to oily residue. The product (**4**) was precipitated in cold diethyl ether (20 ml), suspension was filtered and the precipitation step was repeated three times. H^1-NMR (400 MHz, D_2O, δ, ppm) 3.1 (m, 2H, NH_2-C$\underline{H}_2$-CH_2-S-); 3.29 (t, 2H, NH_2-CH_2-C$\underline{H}_2$-S-); 7.3 (m, 1H, 3'-H, pyridyl); 7.74 (m, 1H, 4 '/ 5'-H, pyridyl), 7.81 (m, 1H, 4' / 5'-H, pyridyl); 8.4 (m, 1H, 6'-H, pyridyl).

*Cholesteryl N-[2-(2-pyridyldisulfonyl)ethyl]carbamate **(5)***

Synthesis of **(5)** was carried out as described in [19] with some modifications (**Fig. 1B step ii)**. To the cholesteryl chloroformate solution (0.4 g, 0.9 mmol) in dry dichloromethane (4 ml), were added the suspension of **(4)** (0.1 g, 0.45 mmol) in dioxane (2 ml) and triethylamine (0.15 mL, 1.1 mmol). The reaction mixture was stirred for 48 h under argon at room temperature. After addition of dichloromethane (20 ml), reaction mixture was washed twice with saturated aqueous $NaHCO_3$ (20 mL) and water (20 mL). The organic phase was dried under anhydrous Na_2SO_4 and evaporated to oily residue. The product **(5)** was purified by silica gel column chromatography (hexane/ethyl acetate, 0-30%) (yield 0.19 g, 71%). H^1-NMR (400 MHz, $CDCl_3$, δ, ppm): 0.69 (s, 3H, H-18/19 cholesterol); 0.87 (d, 3H, H-26/27 cholesterol); 0.89 (d, 3H, H-26/27 cholesterol); 0.93 (d, 3H, H-21 cholesterol); 1.025 (s, 3H, H-18/19 cholesterol); 2.92 (dd, 2H, -NH-C$\underline{H}_2$-CH2-S-,); 3.44 (m, 2H, -NH-CH_2-C$\underline{H}$2-S-,): 4.47 (m, 1H, H-3

cholesterol); 4.88 (t, 1H, -NH-,); 5.35 (d, 1H, H-6 cholesterol); 7.1 (m, 1H, 3'-H, pyridyl); 7.51 (m, 1H, 4 '/ 5'-H, pyridyl), 7.59 (m, 1H, 4' / 5'-H, pyridyl); 8.51 (m, 1H, 6'-H, pyridyl).

Oligonucleotide synthesis

Oligoribonucleotide D20H (**Fig. 1C)** was synthesized on an automatic DNA/RNA ASM-800 synthesizer (Biosset) at 0.4 μmol scale using 2′-O-TBDMS-protected phosphoramidites and solid phase phosphoramidite synthesis protocols [20] optimized for the instrument. Synthesis of 3'-amino modified oligoribonucleotide (N-D20H) was carried out using 3'-PT-Amino-Modifier C6 CPG (Glen Research). At the final step of the synthesis, Thiol-Modifier C6 SS or 5'-Aldehyde-Modifier C2 phosphoramidites were used. Cleavage of oligoribonucleotides from the support and removal of 2′-O-silyl and nucleobase exocyclic amine protecting groups were carried out as described before [13].

Synthesis of lipophilic conjugates with hydrazone bond *(D20HcnCh and N-D20HcnCh)*

Modified with 5'-O-Aldehyde-Modifier C2 phosphoramidite oligoribonucleotides D20H and N-D20H were incubated in 80% acetic acid 1h at room temperature to remove the acetal protecting group, then oligoribonucleotides were precipitated by addition of 2% $NaClO_4$ in acetone and isolated via preparative electrophoresis in 12% polyacrylamide/8M urea gel (acrylamide:N,N′-methylenebisacrylamide 30:0.5, TBE buffer, 10 V/cm) followed by elution with 0.3 M NaOAc (pH 5.2)/0.1% SDS solution and precipitation with ethanol. Purified oligoribonucleotides D20H-CHO and N-D20H-CHO were conjugated with compound **(3) (Fig. 1A steps iv, v)**. For this, the oligoribonucleotides (5 units A_{260}) dissolved in 50μl of 0.1 M NaOAc pH 5.0 were mixed with the same volume of **(3)** (3 mg, 5,2 μmol) in dioxane and incubated 12h at room temperature with permanent stirring. Yield of the products D20HcnCh and N-D20HcnCh was estimated by gel electrophoresis and ethidium bromide staining as a ratio between signals corresponding to product (D20HcnCh or N-D20HcnCh) and initial compound (D20H-CHO or N-D20H-CHO). Cholesterol-conjugated oligoribonucleotides D20HcnCh and N-D20HcnCh were characterized by ESI-TOF-MS analysis (theoretical mass – 12405,8 Da, measured mass – 12405,2 Da) performed by the Proteomics Platform of Esplanade, Strasbourg, France.

Synthesis of lipophilic conjugates with disulfide bond (*D20HssCh and N-D20HssCh****)***

Modified with Thiol-Modifier C6 S-S phosphoramidite (Glen Research) oligonucleotides D20H and N-D20H (5 OU) were treated with 50 mM DTT, 25 mM HEPES-NaOH, pH 8.5 at room temperature for 30 min with permanent stirring, precipitated with 2% $NaClO_4$ in acetone, the pellet was washed with acetone and dried. The reduced 5'-thiol containing

oligonucleotide derivatives D20H-SH and N-D20H-SH **(Fig. 1C)** were purified using Bio-Rad P6 column in 100 mM HEPES-NaOH, pH 8.5, for complete elimination of DTT. Compound **(5)** (2 mg, 3,3 μmol) in dioxane (0.2 ml) was added to 5'-thiol oligonucleotide and incubated overnight at room temperature with permanent stirring **(Fig. 1B steps iii, iv)**, followed by precipitation with 2% $NaClO_4$ in acetone. Cholesterol-conjugated oligoribonucleotides D20HssCh (yield 30%) and N-D20HssCh (yield 45%) (yields were estimated as described above) were isolated via preparative electrophoresis in 12% polyacrylamide/8M urea gel, followed by elution with 0.3 M NaOAc (pH 5.2)/0.1% SDS solution and precipitation with ethanol. The purified D20HssCh and N-D20HssCh were characterized by ESI-TOF-MS analysis (theoretical mass – 12320,4 Da, measured mass – 12321,0 Da).

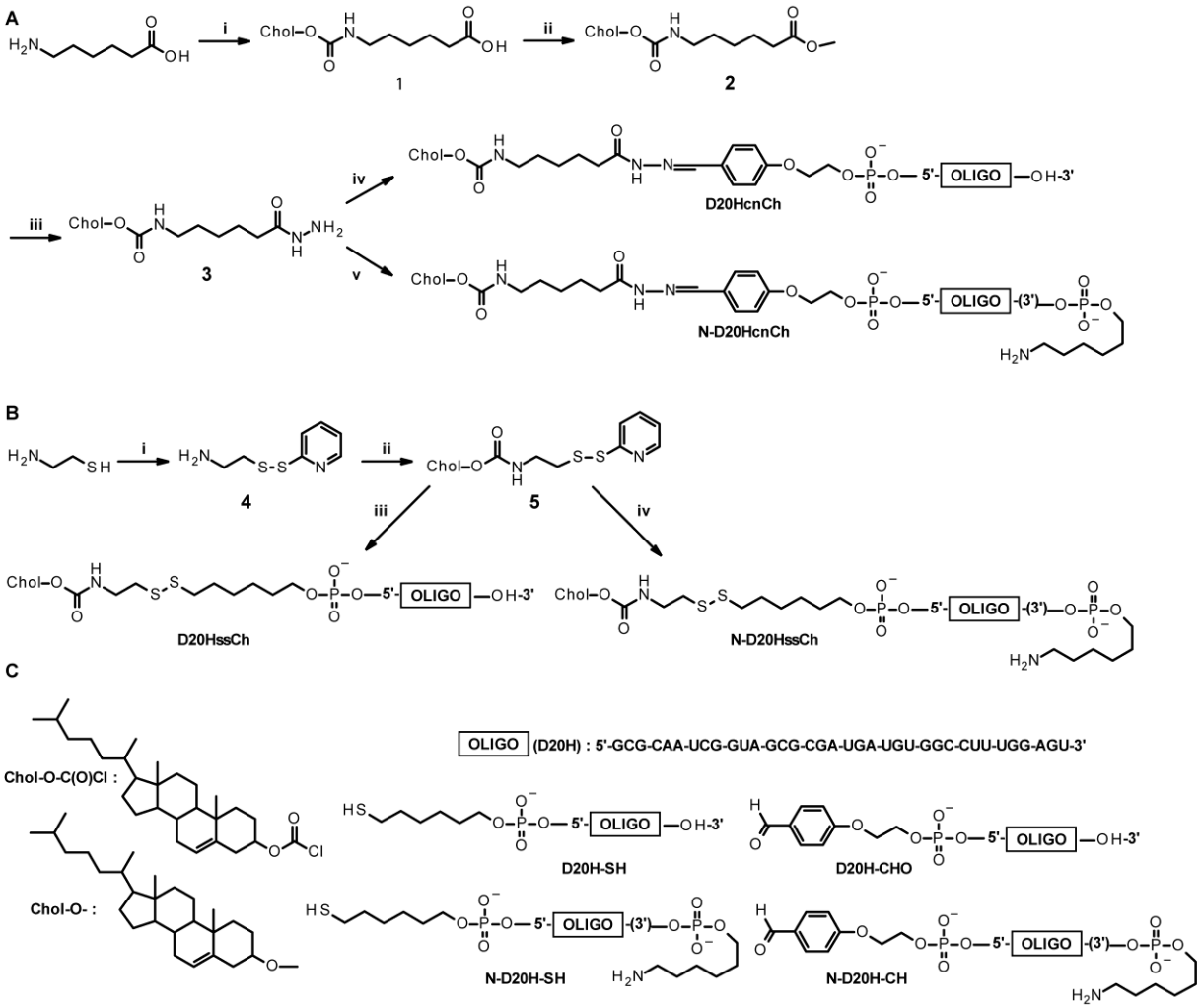

Figure 1. Synthesis of oligoribonucleotides conjugated with cholesterol through cleavable covalent bonds, hydrazone (**A**) and disulfide (**B**). *Reagents:* ***A****, i) $(CH_3)_3SiCl$, Py, 4 ^{O}C; CholOC(O)Cl, Py, r.t.; H_3O+; ii) PCl_3, CH_2Cl_2, argon, 50^{O}C; $MeOH_{abs}$, r.t.; iii) $NH_2NH_2 \cdot H_2O$, MeOH, r.t.; iv)D20H-CHO, 0.1M NaOAc, pH 5.0/dioxane, r.t.; v) N-D20H-CHO, 0.1M NaOAc, pH 5.0/dioxane, r.t.;* ***B****. i) $(PyS)_2$, MeOH/AcOH, r.t.; ii) CholOC(O)Cl, CH_2Cl_2/dioxane/Et_3N, argon, r.t.; iii) D20H-SH, dioxane, r.t.; iv)*

N-D20H-SH, dioxane, r.t. ***C.*** Structure of compounds used for the synthesis.

Synthesis of fluorescently labeled conjugates

Synthesis of fluorescently labeled lipophilic conjugates with ATTO-565 or FITC was carried out as described previously [21]. Briefly, the conjugate containing 3′-terminal aminolinker (N-D20HssCh or N-D20HcnCh) (5 units A_{260}) dissolved in 85 μL of HEPES-NaOH 0.1 M, pH 8.5 was mixed with 15 μL of *N*-succinimidyl esters of ATTO-565 in dry DMSO (5 mg/ml); or (N-D20HcnCh) (1 OU) in 30 μL of HEPES-NaOH 0.1 M, pH 8.5 was mixed with 30 μL of FITC dissolved in dry DMSO (10 mg/ml). Reaction mixture was incubated overnight at room temperature with permanent stirring. The conjugates were precipitated with ethanol as Na+ salts.

Test of the lipophilic conjugates stability

To test of the lipophilic conjugates stability in OptiMem, 20 ng of ATTO-565 labeled D20HcnCh or D20HssCh conjugates were incubated 3 h at 37°C in 25 μl of OptiMem reduced serum medium. To test the hydrazon bond stability, 100 ng of D20HcnCh conjugate was incubated for 2.5, 4, 6, 8 and 24 h at 37°C in 20mM Na-acetate buffer pH 4.6; 5.2 or 5.6 or Na-phosphate buffer pH 6.0; 6.6 or 7.4. Stability of D20HssCh was tested in 20 mM Hepes-NaOH pH 7.4 containing 5mM glutathion (GSH) 3h at 37°C. For complete reduction of the disulfide bond, 20 mM β–mercaptoethanol was added for 15 min at room temperature.

Reaction products were separated on 8M urea – 12% PAGE (AA/bisAA 30:0.5), TBE, stained with Ethidium Bromide and quantified using G-box and GeneTools analysis software (Syngene) or PhosphorImager (Typhoon-Trio, GE Healthcare).

Cell culture and transfection

Homo sapiens bone osteosarcoma 143B cells and primary skin fibroblasts from a patient, bearing mtDNA point mutation in the *ND5* gene (A13514G) at 30% heteroplasmy level [8], were cultivated at 37°C and 5% CO_2 in MEM (Sigma) containing 1 g/l glucose, supplemented with fetal calf serum (Gibco), 100 U/ml penicillin, 100 μg/ml streptomycin, uridine (50 mg/l) and fungizone (2.5 mg/l) (Gibco). For carrier-free transfection with the lipophilic conjugates labeled with ATTO-565, cells (2 cm^2) were washed with PBS, Opti-MEM Reduced Serum medium (Gibco) containing 10 – 100 nM final concentration of conjugates was added and cell were cultivated 15h at 37°C and 5% CO_2, then the medium was changed to MEM. Transfection procedure did not lead to detectable decrease of viability of the cells. Efficiency of transfection was evaluated by flow cytometry using CyFlow® Space (*Partec*), ATTO-565 labeled conjugates was excited at 488nm, and fluorescence emitted at 592 nm. More than

10,000 cells from each sample were analyzed using Flowing Software 2.5.1 (Perttu Terho, Turku Centre for Biotechnology).

Fluorescent confocal microscopy

For confocal microscopy, cybrids cells cultivated in 2 cm^2 chambers slide (Lab-Tek) were transfected with ATTO-565 or FITC labelled RNA-cholesterol conjugates. At different time periods after transfections, living cells were stained with 100 nM MitoTracker Green or Deep Red correspondingly for 30 min at 37°C, washed and imaged in MEM without red phenol. For chloroquine treatment, transfected cells were cultivated in MEM containing 100 μM chloroquine for 5h, then the medium was changed to MEM.

LSM 780 confocal microscope (Zeiss) was used in conjunction with Zen imaging software and images acquired with a Zeiss 63x /1,40 oil immersion objective. The excitation/ emission laser wavelengths were 488 nm (green channel) and 555 nm (red channel). Images were analysed using ImageJ [22] and MosaicSuit plug-in [23].

Heteroplasmy test

Patient fibroblasts were transfected with 1 μM D20HcnCh conjugate for 15h, cultivated 2 days in MEM, then another 15h transfection has been performed. In various post-transfection time periods, cellular DNA was isolated, and heteroplasmy level analysis was performed as described previously [8], using fluorescently labelled primer 5'-FITC-CATACCTCTCACTTCAACCTCC-3' (Eurogentec). Briefly, the heteroplasmy level was analyzed by restriction fragment length polymorphism on a 125-bp PCR fragment where A13514G mutation creates an HaeIII-specific cleavage site. The HaeIII-digested fragments were separated on a 10% PAGE and quantified using PhosphorImager (Typhoon-Trio, GE Healthcare).

Statistical analysis

Results of mitochondrial uptake and heteroplasmy test were statistically processed using the one-way ANOVA, followed by the Duncan's test, values of $p \leq 0.05$ (*), $p \leq 0.001$ (***) were considered to be statistically significant. IBM SPSS software v.22 has been used for analysis. Data are expressed as mean ±S.D. for at least 3 independent experiments.

Results

Lipophilic conjugates of oligoribonucleotides

To establish a carrier-free transfection of human cells with small RNA molecules, we used an anti-replicative RNA (referred to as D20H) targeting a point mutation in ND5 gene,

previously demonstrated to be imported into mitochondria and able to decrease the heteroplasmy level in human cybrid cells and patient fibroblasts [8]. This small RNA was conjugated with cholesterol through a biodegradable disulfide bond (D20HssCh, **Fig**. 1). For this, oligoribonucleotides synthesized according to the phosphoramidite method were 5'-O-thiol-modified and conjugated with cholesteryl N-[2-(2-pyridyldisulfonyl)ethyl]carbamate **(**compound **5, Fig. 1B**). Since the length of the linker between the RNA and lipophilic residue significantly influenced the cellular accumulation of siRNA conjugates [13], we designed a molecule containing 6 carbon atoms, S-S bridge and another two carbon atoms between 5'-nucleotide of RNA and cholesterol residue (**Fig. 2A**). Purified lipophilic oligoribonucleotide was analyzed by ESI-TOF mass spectrometry. The calculated molecular weight was in agreement with the measured value, confirming the structure of the isolated product.

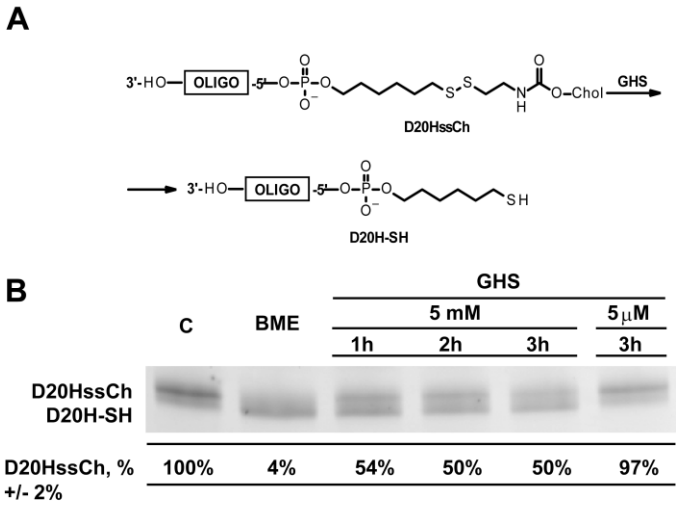

Figure 2. Cleavage of disulfide bond in D20HssCh conjugate in presence of glutathion (GSH). **A**, Structure of D20HssCh conjugate and its reduced form D20H-SH. **B**, Gel electrophoresis analysis of the conjugate treated with GSH as indicated above the panel. Quantification of the portion of D20ssCh (upper band) expressed as mean ±S.D. for 3 independent experiments is shown below the lanes.

Cleavage of the S-S bond by glutathion (GSH) treatment can be detected by separation of molecules bearing or not a cholesterol residue by denaturating PAGE **(Fig. 2B**). After 3h incubation at 37° in buffer containing 5 μM GSH (corresponding to GSH concentration in blood), the S-S bond was not significantly cleaved (**Fig. 2B**). Upon the increase of GSH concentration up to 5 mM (corresponding to GSH concentration in cytosol of mammalian cells [24])**,** S-S bond reduction was detected in 50% of molecules, indicating that the conjugate of oligoribonucleotide with cholesterol through a disulfide bond should be rapidly cleaved after delivery into cytoplasm, thus permitting the mitochondrial import of the RNA moiety.

Another type of biodegradable linker is a hydrazone bond, which can be cleaved in acid conditions of certain cellular compartments including endosomes [15]. To obtain an

optimal balance between the hydrazone bond lability under acidic conditions and stability under neutral conditions, we used the combination of an aromatic aldehyde with an aliphatic acyl hydrazide [15] (**Fig. 1A**). We designed a linker containing 2 carbon atoms, hydrazone bridge and another 6 carbon atoms between 5'-nucleotide of RNA and cholesterol residue.

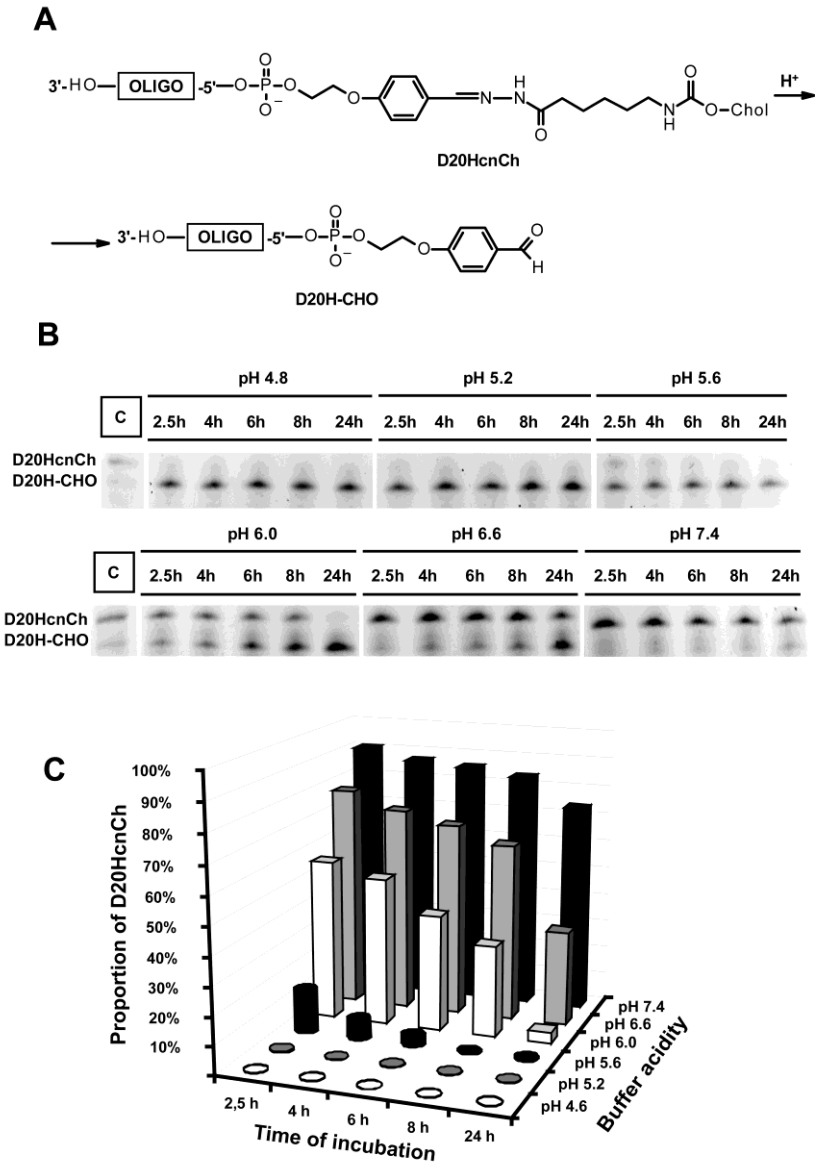

Figure 3. Hydrazone bond cleavage in D20HcnCh conjugate. **A**, Structure of D20HcnCh conjugate and its cleaved form D20H-CHO. **B**, Gel electrophoresis analysis of the hydrolysis products after incubation of the conjugate at various pH during 2.5, 4, 6, 8 and 24 hours (as indicated above the panels). Bands corresponding to the full size conjugate (upper band) and the product of its acid hydrolysis (lower band) are indicated at the left. **C**, Quantification of the full size conjugate (%, axis Y) depending on pH and the time of incubation.

For this, hydrazino 6- (cholesteryloxycarbonylamino) hexanoate (compound **3, Fig. 1A**) was synthesized and conjugated to D20H RNA. Lability of the resulted hydrazone bond was tested at various pH conditions, demonstrating that the hydrazone link is stable at pH 6.6 and above, while at pH 6.0 it was completely cleaved in 24h. At more acidic pH (5.6 and below), cholesterol residue was quickly cut from oligoribonucleotide (50% and 90% of molecules

were hydrolyzed in 2.5 hours at pH 6 and 5.6 respectively) (**Fig. 3**). Therefore, the conjugate of oligoribonucleotide with cholesterol through a hydrazone bond (referred to as D20HcnCh) should be stable during the cell transfection procedure (pH 7.4), and then would be cleaved inside the endosomes, thus facilitating the release and further mitochondrial import of the RNA moiety.

Cellular uptake of lipophilic conjugates

To detect and quantify the cellular uptake of RNA conjugated with cholesterol, 3'-end of the oligoribonucleotide was labeled with fluorescent compound ATTO-565. Carrier-free transfection of cultured human cells was performed by incubation of cells with increasing concentrations of RNA conjugated with cholesterol. Efficiency of transfection was measured using cytofluorometry (**Fig. 4 A,B**).

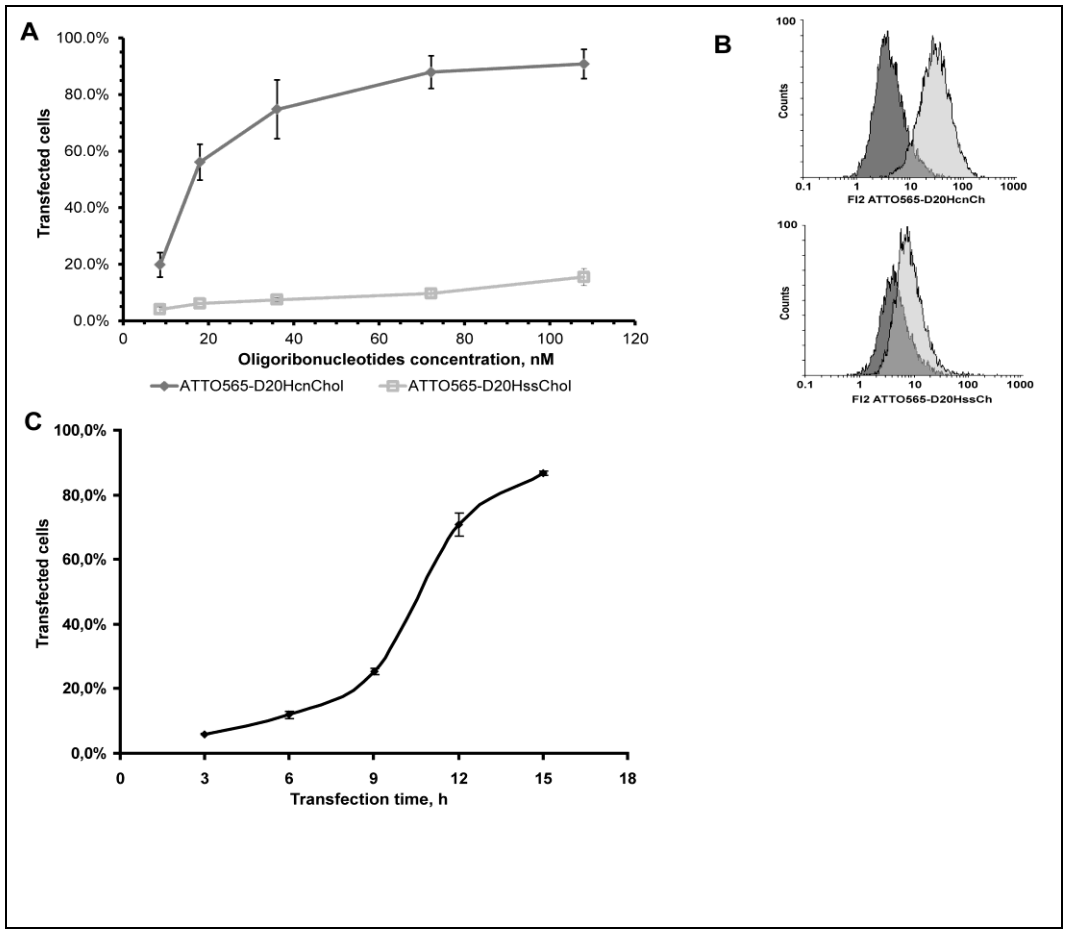

Figure 4. Cellular uptake of ATTO-labeled lipophilic conjugates estimated by flow cytometry. **A**, the percentage of ATTO-positive cells in the population after 15h incubation with increased concentrations of conjugates (indicated below the graphs). **B**, an example of flow cytometry analysis, cells were incubated 15h with 70 nM ATTO-D20HcnCh (above) or ATTO-D20HssCh (lower panel). In dark gray, signal corresponding to auto-fluorescence of non-transfected cells. **C**, the percentage of ATTO-positive cells in the population after incubation with 70 nM D20HcnCh during

various periods of time (indicated below). More than ten thousand events were counted in each sample; mean values from three independent experiments are presented.

Cellular delivery of RNA conjugated with cholesterol through a disulfide bond (D20HssCh) was rather inefficient, the fluorescence exceeding the maximum level of cell auto-fluorescence was detected in less than 10% of cells. In contrast to poor uptake obtained for D20HssCh, D20H RNA conjugated through a hydrazone bond (D20HcnCh) was rather efficiently internalized by cells. Percentage of transfected cells reached a plateau of 90±2% after 15h of incubation with 70 nM D20HcnCh (**Fig. 4C**). Fluorescent confocal microscopy images also demonstrated a very low internalization of D20HssCh molecules and efficient accumulation of D20HcnCh in the cytoplasm of the transfected cells (**Fig**. **5**).

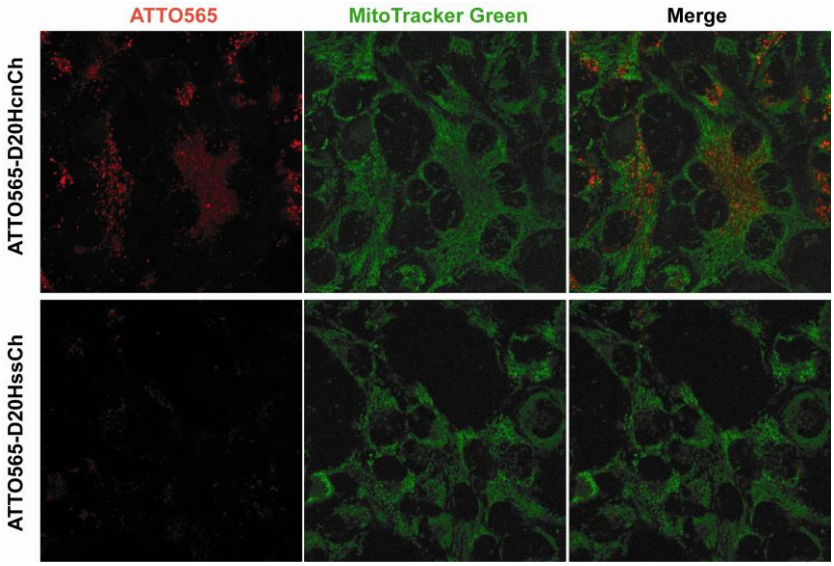

Figure 5. Cellular uptake of ATTO-labeled lipophilic conjugates analyzed by fluorescent confocal microscopy after 15h incubation with ATTO-D20HcnCh or ATTO-D20HssCh as indicated at the left. Mitochondria were stained with MitoTracker Green (indicated above the panel).

To explain the low level of D20HssCh delivery, we tested the stability of conjugates in conditions used for cells transfection. After 3h of incubation at 37^{o}C in Opti-MEM medium, more than 70% of D20HssCh conjugate was cleaved, whereas D20HcnCh demonstrated high stability in the same conditions (**Fig. 6A, B)**. We hypothesized that RNA cleavage occurs due to reduction of the disulfide bond by components of the medium, followed by coordination of metal cations by free thiol groups. In previous studies, conjugation of oligodeoxyribonucleotides or siRNA to cholesterol with a cleavable disulfide linker did not cause a degradation of the oligonucleotide [25, 26]. We suppose that the secondary structure of the antireplicative RNA and the 5'-end position of the disulfide linker (**Fig. 6C)** can result in a close proximity of the thiol group to the single-stranded RNA region, thus facilitating the RNA cleavage induced by metal cations [27] . Addition of 2 mM EDTA completely abolished

the RNA degradation, supporting our hypothesis of the D20Hsh metal-dependent cleavage. Therefore, in our case, the disulfide bond was rapidly reduced during the cells transfection procedure, promoting the subsequent degradation of the RNA moiety. Further experiments were performed with cells transfected with D20HcnCh conjugate.

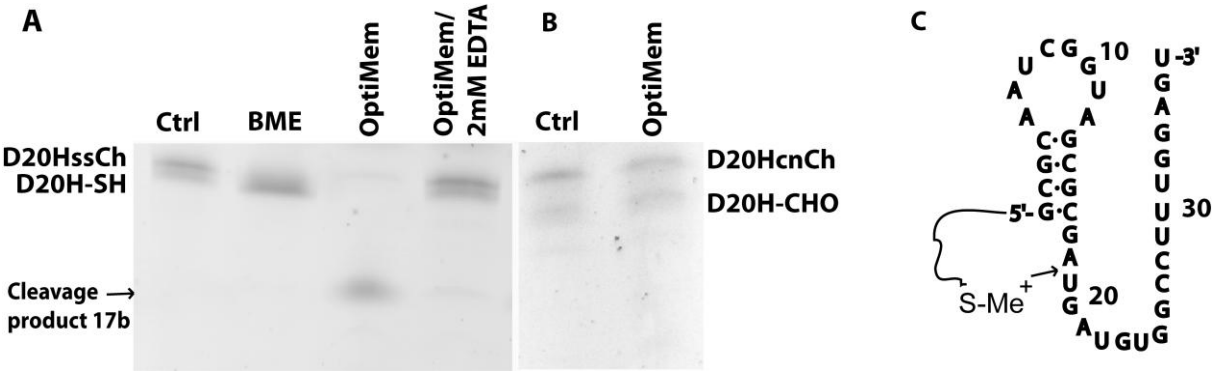

Figure 6. Stability of the lipophilic conjugates in OptiMEM media. Gel electrophoresis analysis of D20HssCh (**A**) and D20HcnCh (**B**) incubated 3h at 37°, conditions indicated above the panels. Ctrl, control, conjugates incubated in water; BME, treatment with 20 mM β–mercaptoethanol. **C**, predicted structure of reduced D20Hsh molecule, Me^{+}, divalent cation bound to the free thiol group which can induce RNA cleavage at the position indicated by an arrow, producing a 17b RNA fragment.

Mitochondrial targeting and anti-replicative capacity of D20H RNA

We used optimized conditions for the carrier-free cell transfection with D20HcnCh conjugate (15h of incubation with 70 nM D20HcnCh) to check if the RNA-component of the internalized conjugate can be targeted to mitochondria. For this, we used confocal laser scanning microscopy of living cells. D20HcnCh was labeled with fluorescein (FITC) at 3'-end, mitochondrial network stained by MitoTracker Deep Red, and co-localization of fluorescent signals had been quantified and statistically analyzed (**Fig. 7**). The data clearly show that the FITC-labeled molecules are partially (13±3 % of the cellular pool) addressed to mitochondria 20h post-transfection, the co-localization stayed at the same level 45h post-transfection and significantly decreased after 70h, indicating on the RNA degradation (**Fig. 7 A, B)**. Control experiments with FITC only did not demonstrate significant co-localization with mitochondria (1-2%, not shown).

To check the impact of the hydrazone bond cleavage, which was anticipated to occur in acid conditions inside the endosomes, facilitating the release and mitochondrial import of RNA, we treated the transfected cells with chloroquine, an agent that prevents endosomal acidification, commonly used to study the role of endosomal pH in cellular processes [28]. After 5h of chloroquine treatment, the level of D20H co-localisation with mitochondria was significantly decreased (**Fig. 7A,C**). This indicates that the increased endosomal pH,

preventing the D20HcnCh hydrazone bond cleavage, resulted in the decreased amount of D20H RNA molecules released from the membrane-bound conjugate with cholesterol and therefore accessible for the mitochondrial targeting.

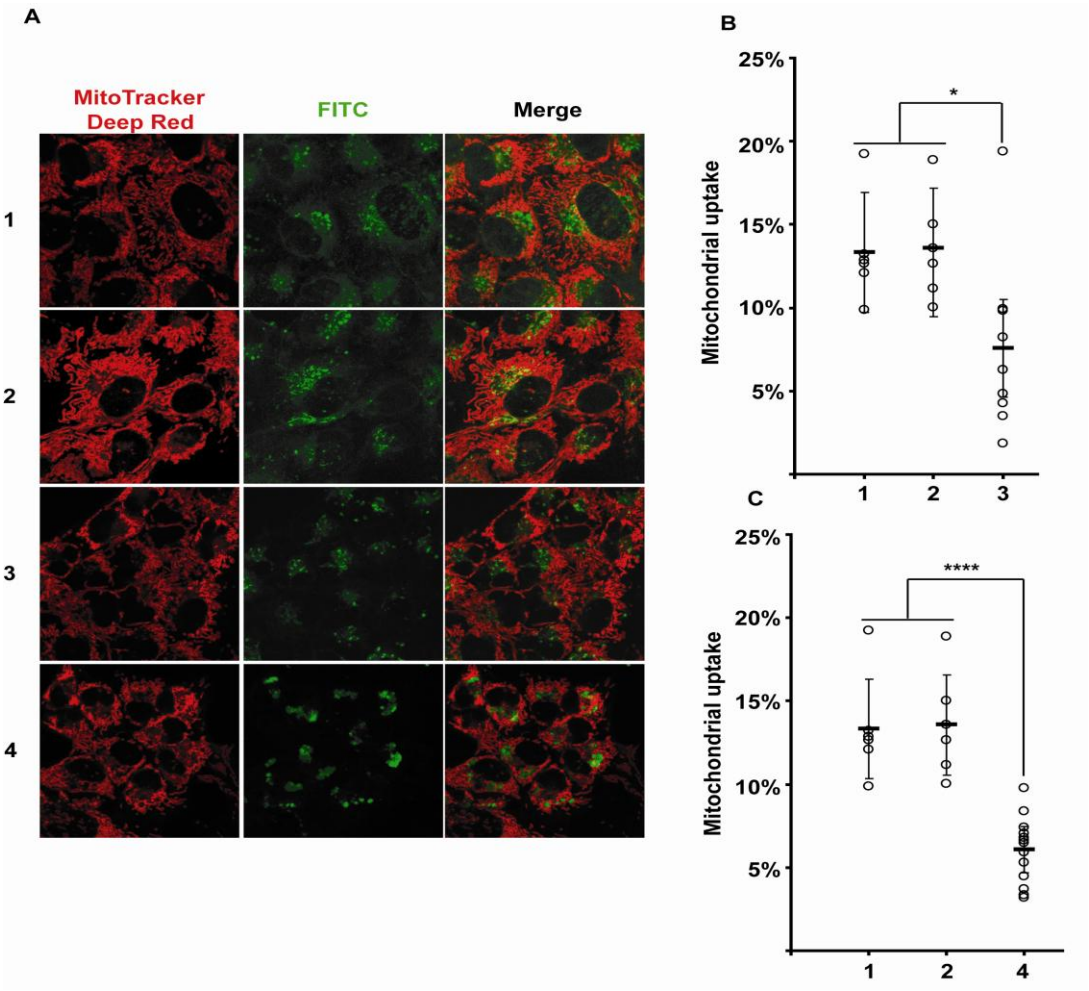

Figure 7. Mitochondrial targeting of D20H RNA evaluated by fluorescent confocal microscopy. **A**, confocal microscopy images of 143B cells incubated with FITC-D20HcnCh (green signal), 20h (**1**), 45h (**2**) and 70h (**3**) post-transfection; (**4**), cells were incubated with FITC-D20HcnCh for 15h, treated with Chloroquine for 5h and analyzed 45h post-transfection. Mitochondrial network was visualized by MitoTracker DeepRed staining. **B** and **C**, quantification of RNA co-localization with mitochondria, estimated as the percentage of green fluorescence signal co-localized with red fluorescence for 6–14 optical sections. The data were statistically processed using the one-way ANOVA, followed by the Duncan's test. Significant differences between cells: *, $p<0.05$; ****, $p<0.001$.

To prove that the released D20H RNA still possessed the anti-replicative activity inside the mitochondria, we performed the carrier-free transfection of patient fibroblasts bearing the pathogenic point mutation in ND5 gene of mtDNA [8]. In various post-transfection time periods, cellular DNA was isolated, and the proportion between normal and mutant mitochondrial genomes (so called heteroplasmy level) was measured by cleavage of the PCR amplicon (**Fig. 8**). A small but significant decrease of the mutant mtDNA proportion has been

detected in the transfected fibroblasts, but not in the control cells cultivated in the same conditions. These data indicate that the conjugation with cholesterol can be useful for a carrier-free delivery of therapeutic anti-replicative RNA into mitochondria of human cells.

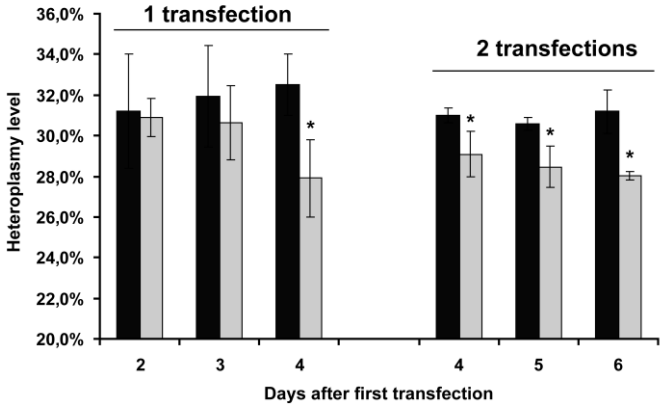

Figure 8. The effect of D20HcnCh on heteroplasmy level in transfected patient fibroblasts bearing A13514G mutation in mtDNA. Time dependence of heteroplasmy level during 6 days (as indicated below the graphs) after one or two consecutive transfections with D20HcnCh conjugate (shown in gray) or in the control cells cultivated in the same conditions without transfection (in black). Data are expressed as mean ±S.D. for 3–4 independent experiments. Significant differences between control and transfected cells were calculated by one-way ANOVA, followed by Duncan's test (*, $p<0.05$).

Discussion

RNA therapeutics is an emerging class of innovative medicine. In recent years, significant progress has been made to overcome some of the obstacles associated with *in vivo* delivery of RNA [29]. Lipid nanoparticles represent one of the most advanced technological platforms [30], together with the rapidly developing approach of molecular conjugates, as triple acetyl-galactosamine conjugates, combination of backbone neutralization with cell-penetrating peptides [31], or lipophilic conjugates [12, 32]. A variety of lipophilic moieties can be conjugated to siRNAs to improve the *in vivo* uptake, the best studied one being cholesterol. Mechanistically, cholesterol-modified siRNAs interact with serum lipoprotein particles and the uptake is dependent upon cellular lipoprotein and other *trans*membrane receptors [12]. Recently reported data demonstrate that the adsorption of siRNA lipophilic conjugates on the cell surface and their subsequent transport into the cells could occur *via* the mechanism of endocytosis. It was suggested that two main factors might determine the efficacy of adsorption of the conjugates on the cell surface: the hydrophobicity of the conjugates and the distance between negatively charged cellular membrane and anionic siRNA [13]. The long aliphatic linker in the conjugate structure provides an optimal distance between the cellular membrane and siRNA moiety, along with an increase of the hydrophobicity of the conjugates. Taking into account these data, we synthesized mitochondrially imported RNAs conjugated to cholesterol through the linker containing 8 carbon atoms.

Another important point is that chemical modifications introduced into RNA molecules should not interfere with their sub-cellular localisation and therapeutic function. In case of siRNA duplexes, lipophilic residue can be conjugated to the sense strand, which is destroyed upon the cell delivery by RISC complex. For anti-replicative RNAs, expected to be mitochondrially targeted and to interact with mutant mitochondrial genomes stalling their replication [4], the cholesterol residue, improving the cellular uptake, can also create an obstacle for the mitochondrial import. In fact, human mitochondria possess a system facilitating the transport of cholesterol from the outer mitochondrial membrane to the inner one. This transport is necessary for cholesterol metabolization to pregnenolone, the precursor of all steroid hormones [33]. Translocator protein of the outer mitochondrial membrane TSPO consists of five *trans*membrane helices forming a channel-like structure that may accommodate the import of lipophilic molecules into mitochondria and contains a recognition motif with high affinity to cholesterol [34]. Therefore, the cholesterol residue can be recognized by TSPO and translocated through the outer mitochondrial membrane. In this case, RNA molecule conjugated with cholesterol would be trapped on the outer membrane and, probably, could not be addressed into mitochondrial matrix. To avoid thisproblem, we introduced a cleavable linker between RNA and cholesterol residue. We expected that the linkers (disulfide or hydrazone bonds) should be stable during cell transfection procedure and cleaved upon internalizing of the conjugate in the cytoplasm [15]. Mammalian cells uptake of extracellular macromolecules proceeds through endocytosis, leading (for the most of endocytosis pathways) to formation of vesicle-like structures that fuse with early endosomes characterised by a reduced pH (6.0–6.6, compared to a physiological pH 7.2–7.4) [35]. The pH drops further during endosomal processing, reaching 5.0 at the late endosomal stage. Therefore, we supposed that the hydrazone bond between RNA and cholesterol moieties would be cleaved inside the endosome, while the disulfide bond should be cleaved after release of the conjugate into the cytoplasm. In both cases, this should permit the mitochondrial targeting of the therapeutic RNA.

Unexpectedly, our data revealed a very low level of cellular uptake for RNA conjugated with cholesterol through a disulfide bond (D20HssCh) compared to RNA conjugated through a hydrazone bond (D20HcnCh). This low uptake was a consequence of a cleavage of the disulfide bond in the medium used for cell transfection (OptiMEM), followed by a rapid RNA degradation (**Fig. 6**). This is a first demonstration of a low stability of structured RNA conjugated with cholesterol through a disulfide bond so far. Thus, the

secondary structure of antireplicative RNAs should be taken into account for further design of conjugates with disulfide linkers.

Hydrazone bonds demonstrated an improved stability in the transfection media, thus assuring an efficient carrier-free cellular uptake of the conjugated molecule D20HcnCh. The level of its consequent co-localisation with mitochondria was estimated as 13±3 % of the D20H cellular pool (Fig. 7). We suppose that this value is limited by the endosomal escape of the D20H RNA after the hydrazone bond cleavage in acidic conditions. However, the treatment of transfected cell with chloroquine, one of endosomal escape agents, supposed to facilitate the disruption of the endosomal membrane due to proton sponge mechanism [36], decreased the mitochondrial targeting of D20H RNA (Fig. 7). This result indicates that the conjugated molecules D20HcnCh are anchored in the endosomal membranes due to cholesterol residue, and the RNA component cannot be released at neutral pH even upon the disruption of endosomes.

Noteworthy, the moderate mitochondrial import of D20H RNA still allowed detection of its anti-replicative activity. Even the small decrease of heteroplasmy level (Fig. 8) can be important to obtain a curative effect of mitochondrial dysfunctions in human cells, since only high levels of mutations in human mtDNA become pathogenic [6], while a small reduction of the mutant DNA load can provide significant clinical improvement [37]. We believe that the present study represents a further step towards the development of RNA therapeutics against incurable mitochondrial diseases.

Acknowledgements

The authors are grateful to Dr. Agnès Rötig (*Hôpital Necker-Enfants Malades, Paris)* for providing the patient fibroblasts, to Jérôme Mutterer (*IBMP, Strasbourg*) for helpful assistance in confocal microscopy, to Philippe Wolf (*IBMC, Strasbourg*) for ESI-TOF-MS analysis, to Anne-Marie Heckel for excellent technical assistance and to Dr. Anna Smirnova and Dr. Alexandre Smirnov for helpful discussions.

This work has been published under the framework of the LABEX ANR-11-LABX-0057_MITOCROSS and is supported by the state managed by the French National Research Agency as part of the Investment for the Future program. The work was also supported by CNRS (Centre National de Recherche Scientifique); University of Strasbourg, the LIA (International Associated Labortory) ARN-mitocure and by the grant number 14-14-00697 of the Russian Research Foundation (RSCF). ID was supported by ACRUS-SUPRACHEM and MitoCross PhD fellowships.

References

1. Burnett, JC, and Rossi, JJ (2012). RNA-based therapeutics: current progress and future prospects. *Chemistry & biology* **19**: 60-71.
2. Tavernier, G, Andries, O, Demeester, J, Sanders, NN, De Smedt, SC, and Rejman, J (2011). mRNA as gene therapeutic: how to control protein expression. *J Control Release* **150**: 238-247.

3. Kolesnikova, O, *et al.* (2010). Selection of RNA aptamers imported into yeast and human mitochondria. *RNA* **16**: 926-941.
4. Comte, C, *et al.* (2013). Mitochondrial targeting of recombinant RNAs modulates the level of a heteroplasmic mutation in human mitochondrial DNA associated with Kearns Sayre Syndrome. *Nucleic Acids Res* **41**: 418-433.
5. Ruiz-Pesini, E, *et al.* (2007). An enhanced MITOMAP with a global mtDNA mutational phylogeny. *Nucleic Acids Res* **35**: D823-828.
6. Wallace, DC (2010). Mitochondrial DNA mutations in disease and aging. *Environmental and molecular mutagenesis* **51**: 440-450.
7. Taylor, RW, and Turnbull, DM (2005). Mitochondrial DNA mutations in human disease. *Nat Rev Genet* **6**: 389-402.
8. Tonin, Y, *et al.* (2014). Modeling of antigenomic therapy of mitochondrial diseases by mitochondrially addressed RNA targeting a pathogenic point mutation in mitochondrial DNA. *J Biol Chem* **289**: 13323-13334.
9. Khvorova, A, Osborn, MF, and Hassler, MR (2014). Taking charge of siRNA delivery. *Nat Biotechnol* **32**: 1197-1198.
10. Lv, H, Zhang, S, Wang, B, Cui, S, and Yan, J (2006). Toxicity of cationic lipids and cationic polymers in gene delivery. *J Control Release* **114**: 100-109.
11. Winkler, J (2013). Oligonucleotide conjugates for therapeutic applications. *Ther Deliv* **4**: 791-809.
12. Wolfrum, C, *et al.* (2007). Mechanisms and optimization of in vivo delivery of lipophilic siRNAs. *Nat Biotechnol* **25**: 1149-1157.
13. Petrova, NS, *et al.* (2012). Carrier-free cellular uptake and the gene-silencing activity of the lipophilic siRNAs is strongly affected by the length of the linker between siRNA and lipophilic group. *Nucleic Acids Res* **40**: 2330-2344.
14. Letsinger, RL, Zhang, GR, Sun, DK, Ikeuchi, T, and Sarin, PS (1989). Cholesteryl-conjugated oligonucleotides: synthesis, properties, and activity as inhibitors of replication of human immunodeficiency virus in cell culture. *Proc Natl Acad Sci U S A* **86**: 6553-6556.
15. West, KR, and Otto, S (2005). Reversible covalent chemistry in drug delivery. *Curr Drug Discov Technol* **2**: 123-160.
16. Yamada, C, Khvorova, A, Kaiser, R, Anderson, E, and Leake, D (2013). Duplex oligonucleotide complexes and methods for gene silencing by RNA interference. Google Patents.
17. Tognolini, M, *et al.* (2012). Structure-activity relationships and mechanism of action of Eph-ephrin antagonists: interaction of cholanic acid with the EphA2 receptor. *ChemMedChem* **7**: 1071-1083.
18. Zugates, GT, Anderson, DG, Little, SR, Lawhorn, IE, and Langer, R (2006). Synthesis of poly(beta-amino ester)s with thiol-reactive side chains for DNA delivery. *J Am Chem Soc* **128**: 12726-12734.
19. Sugahara, M, Uragami, M, Yan, X, and Regen, SL (2001). The structural role of cholesterol in biological membranes. *J Am Chem Soc* **123**: 7939-7940.
20. Bellon, L (2001). Oligoribonucleotides with 2'-O-(tert-butyldimethylsilyl) groups. *Curr Protoc Nucleic Acid Chem* **Chapter 3**: Unit 3 6.
21. Dovydenko, I, *et al.* (2015). Mitochondrial targeting of recombinant RNA. *Methods Mol Biol* **1265**: 209-225.
22. Schneider, CA, Rasband, WS, and Eliceiri, KW (2012). NIH Image to ImageJ: 25 years of image analysis. *Nat Methods* **9**: 671-675.
23. Rizk, A, *et al.* (2014). Segmentation and quantification of subcellular structures in fluorescence microscopy images using Squassh. *Nature protocols* **9**: 586-596.

24. Hwang, C, Sinskey, AJ, and Lodish, HF (1992). Oxidized redox state of glutathione in the endoplasmic reticulum. *Science* **257**: 1496-1502.
25. Boutorine, AS, and Kostina, EV (1993). Reversible covalent attachment of cholesterol to oligodeoxyribonucleotides for studies of the mechanisms of their penetration into eucaryotic cells. *Biochimie* **75**: 35-41.
26. Chen, Q, *et al.* (2010). Lipophilic siRNAs mediate efficient gene silencing in oligodendrocytes with direct CNS delivery. *J Control Release* **144**: 227-232.
27. Forconi, M, and Herschlag, D (2009). Metal ion-based RNA cleavage as a structural probe. *Methods Enzymol* **468**: 91-106.
28. Rutz, M, *et al.* (2004). Toll-like receptor 9 binds single-stranded CpG-DNA in a sequence- and pH-dependent manner. *Eur J Immunol* **34**: 2541-2550.
29. de Fougerolles, AR (2008). Delivery vehicles for small interfering RNA in vivo. *Hum Gene Ther* **19**: 125-132.
30. Hope, MJ (2014). Enhancing siRNA delivery by employing lipid nanoparticles. *Ther Deliv* **5**: 663-673.
31. Meade, BR, *et al.* (2014). Efficient delivery of RNAi prodrugs containing reversible charge-neutralizing phosphotriester backbone modifications. *Nat Biotechnol* **32**: 1256-1261.
32. Raouane, M, Desmaele, D, Urbinati, G, Massaad-Massade, L, and Couvreur, P (2012). Lipid conjugated oligonucleotides: a useful strategy for delivery. *Bioconjug Chem* **23**: 1091-1104.
33. Miller, WL, and Bose, HS (2011). Early steps in steroidogenesis: intracellular cholesterol trafficking. *J Lipid Res* **52**: 2111-2135.
34. Jaremko, L, Jaremko, M, Giller, K, Becker, S, and Zweckstetter, M (2014). Structure of the mitochondrial translocator protein in complex with a diagnostic ligand. *Science* **343**: 1363-1366.
35. De Haes, W, Van Mol, G, Merlin, C, De Smedt, SC, Vanham, G, and Rejman, J (2012). Internalization of mRNA lipoplexes by dendritic cells. *Mol Pharm* **9**: 2942-2949.
36. Varkouhi, AK, Scholte, M, Storm, G, and Haisma, HJ (2011). Endosomal escape pathways for delivery of biologicals. *J Control Release* **151**: 220-228.
37. Picard, M, *et al.* (2014). Progressive increase in mtDNA 3243A>G heteroplasmy causes abrupt transcriptional reprogramming. *Proc Natl Acad Sci U S A* **111**: E4033-4042.